Hyperfine Interact (2018) 239:15
https://doi.org/10.1007/s10751-018-1491-5

# Structural and Mössbauer study of nanoparticles $CoFe_2O_4$ prepared by sol-gel auto-combustion and subsequent sintering

**M. Al-Maashani**[1] · **A. M. Gismelseed**[1] ·
**K. A. M. Khalaf**[2] · **Ali A. Yousif**[1] · **A. D. Al-Rawas**[1] ·
**H. M. Widatallah**[1] · **M. E. Elzain**[1]

**Abstract** Single-phased nanocrystalline Cobalt ferrite ($CoFe_2O_4$) have been synthesized by sol-gel auto-combustion method. The prepared sample was divided into four different samples (auto-combustion (S1), 400 °C (S2), 600 °C (S3), and 1000 °C (S4)). The effect of sintering temperature on the structure, and morphology, were subsequently evaluated by X-ray diffraction (XRD), Scanning Electron Microscopy (SEM), Transmission Electron Microscopy (TEM). The hyperfine Interactions of all samples were studied using Mössbauer Spectroscopy (MS). No significant changes noticed in lattice constant (a), and the crystallite size was found to increase with sintering temperature which can be attributed to the grain growth of the particles. SEM shows an increase in the grain size and crystallinity as the sintering temperature increases, and the particles are cubic-like for S4. The particle size of each sample was determined using TEM and were in the range of 10–70 nm for the first three samples S1, S2, and S3, and increased beyond the nano-sized limit for S4 sample. The $^{57}$Fe Mössbauer spectra at 295 K and 78 K showed two sets of magnetic hyperfine patterns for all the four samples, indicating the presence of $Fe^{3+}$ in both A and B-sites, with superimposed doublet in each of S1 and S2 samples. This doublet shows a significant reduction in intensity with increasing the sintering temperature. The existence of the doublet at 78 K suggests that the blocking temperature is below 78 K temperature. From the intensity of the $Fe^{3+}$ sites and assumed site occupancies of the $Co^{2+}$ ions, it may be deduced that the paramagnetic doublet is associated with octahedral site.

---

This article is part of the Topical Collection on *Proceedings of the International Conference on the Applications of the Mössbauer Effect (ICAME 2017), Saint-Petersburg, Russia, 3–8 September 2017*
Edited by Valentin Semenov

✉ M. Al-Maashani
s81088@student.squ.edu.om

[1] Department of Physics, College of Science, Sultan Qaboos University, P.O. Box 36, Code 123, Muscat, Oman

[2] Department of Mathematical and Physical Sciences, College of Arts and Sciences, University of Nizwa, P.O. Box 33, Code 616, Muscat, Oman

**Keywords** Sol gel auto-combustion · Ferrites · Sintering temperature · Mössbauer spectroscopy

## 1 Introduction

The spinel ferrites are ferrimagnetic oxides with their magnetic cations forming two sublattices, namely the tetrahedral (A) and the octahedral [B] crystallographic sites. The structure of the ideal spinel consists of a cubic close-packed array of anions, with one eighth of the tetrahedral and one half of the octahedral interstices occupied by cations, so that the cation to anion ratio is 3:4 [1]. The structural and magnetic environments of these two sites are quite different and are very sensitive to the chemical compositions, preparation sintering temperature and sintering time. Also the type and the amount of cations substitution have very strong effect on the properties. That means it is possible to change the relative strengths of the exchange interactions in spinels by changing the type of the magnetic ions as well as by selective substitution of non-magnetic atoms on the tetrahedral and octahedral sites which lead to interesting spin configurations. Cobalt ferrite has become an ingredient in the formation of metallic/magnetic nano-composites due to the observations of a wide range of magnetic, electric and other novel properties in its derivatives [2, 3]. Recently Waje et al. [4] reported that $Co_{0.5}Zn_{0.5}$ $Fe_2O_4$ nanoparticles, prepared by mechanical alloying and sintering show a constant value of permittivity within a measured frequency range but vary with sintering temperature. However, in general the permeability values vary with both frequency and sintering temperature. Xiangdong Meng et al. [5] reported Mössbauer study of cobalt ferrite nanocrystals substituted with rare-earth $Y^{3+}$ ions synthesized by the sol–gel auto-combustion method. They observed that as the concentration of doped Y increases, $Co^{2+}$ ions migrate to A-sites, leading to an increase in the concentration of $Fe^{3+}$ in B-sites. The superparamagnetism was observed for all the samples with different Y concentrations. The magnetic properties of cobalt ferrite nanoparticles are strongly dependent on their size. In the present paper, the structural and Mössbauer studies of nanocrystalline cobalt ferrite in relation to sintering temperature were investigated.

## 2 Experimental methods

Nano particles of cobalt ferrite were synthesized by the sol-gel auto- combustion method as described in [6]. XRD data were recorded on a Philips diffractometer (model pw 1820), using Cu-K$\alpha$ radiation. Mössbauer spectra were obtained at 295 K and 78 K on a powdered sample using a constant acceleration Mössbauer spectrometer with 50 mCi $^{57}$Co in Rh source. The low temperature measurement was performed using a liquid nitrogen flow cryostat. The spectrometer was calibrated with $\alpha$-Fe foil spectrum at 295 K. The measured data were analyzed using a non-linear least-square fitting program assuming Lorentzian lines.

## 3 Results and discussion

The XRD patterns of $CoFe_2O_4$ nanoparticles at different sintering temperatures auto-combustion, 400 °C, 600 °C and 1000 °C are depicted in Fig. 1 and are typical of spinel structure. Comparing the XRD pattern with the standard data (JCPDS PDF card No. 22-1086), the formation of cobalt ferrite nanoparticles was confirmed for all samples, and no

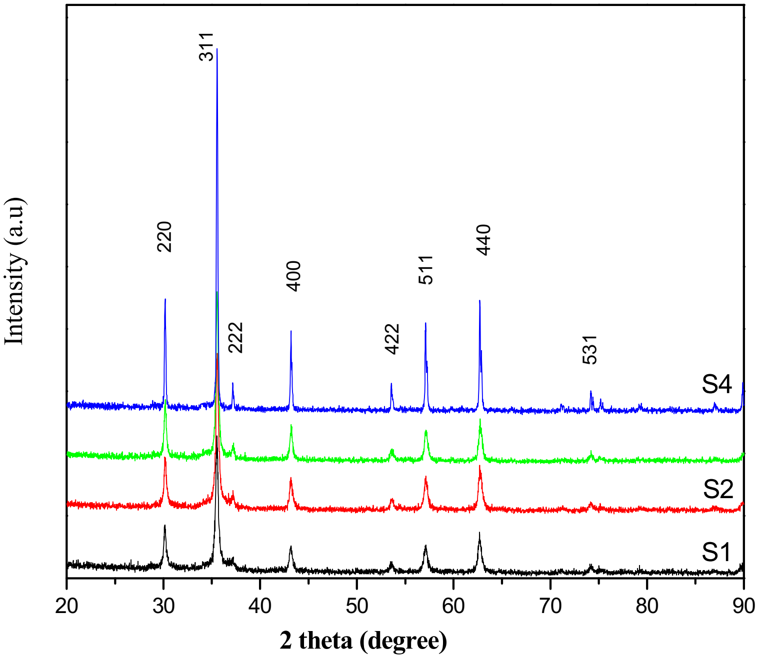

**Fig. 1** XRD patterns of $CoFe_2O_4$ for the four samples

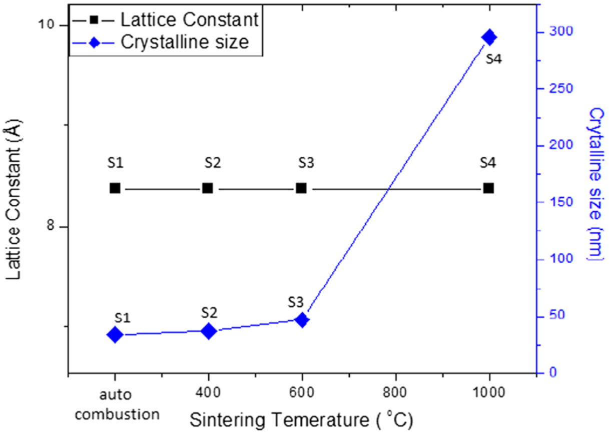

**Fig. 2** Lattice constant and crystallite size for the four samples

other peaks were observed. The diffraction peaks are broad for the first two samples S1 and S2, because of the nanometer size of the crystallite which confirmed by SEM results and Mössbauer spectroscopy. The samples sintered at 600 °C (S3) and 1000 °C (S4) showed very sharp peaks, indicating more crystalline at these temperature.

As shown in Fig. 2, the crystallite size obtained was observed to increase with increasing the sintering temperature. It has been reported that the sintering process generally decreases

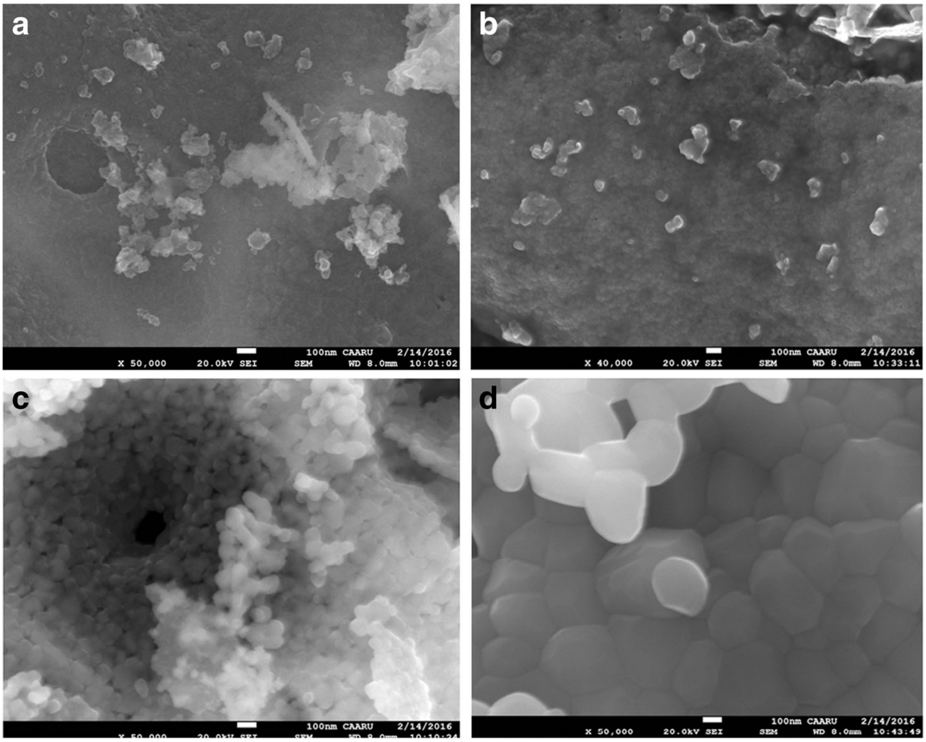

**Fig. 3** The SEM images for the four samples **a** S1, **b** S2, **c** S3, **d** S4

lattice defects and strain, but the applied Sol-Gel technique can cause the coalescence of smaller grains, resulting in an increased of average grain size for the nanoparticles [6]. Calculated values of lattice parameter of cobalt ferrite samples shown in Fig. 2 were in close agreement with previously measured data [7].

The SEM surface morphology images for the all four samples are shown in Fig. 3. The images show that the sample surfaces consist of nanostructured powders, i.e. microparticles resulting from a 3D packing of nanocrystalline grains and composed of approximately cubic/spherical stacked grains of about (10 nm $\sim$ 70 nm) for the samples prepared under auto-combustion condition Fig. 3a and sintering at 400 °C Fig. 3b, which means some particles under superparamagnetic limit (14 nm) as confirmed by the existing doublet in the Mössbauer spectra for these two samples (will be discussed below). The influence of the sintering temperature on the particle size is clear after 600 °C Fig. 3c, it exceeds the nanosize limit (100 nm) at 1000 °C Fig. 3d, with around 200 nm which means that the bulk cobalt ferrite is reached. The TEM image (Fig. 4a) taken for sample under auto-combustion condition shows that the particles have a distribution in their size ranging from 10–50 nm with different shapes cubic, spherical, elliptical, and small particles [8]. Above sintering temperature at 400 °C, the small particles seem to aggregate to form larger particles. Images for samples sintered at 600 °C (S3) and 1000 °C (S4) Fig. 4c and d respectively show large particles with size range between 80–200 nm. In general, the increase in sintering temperature starts to enlarge relatively the size of the particles, as well as affect the particle's shape.

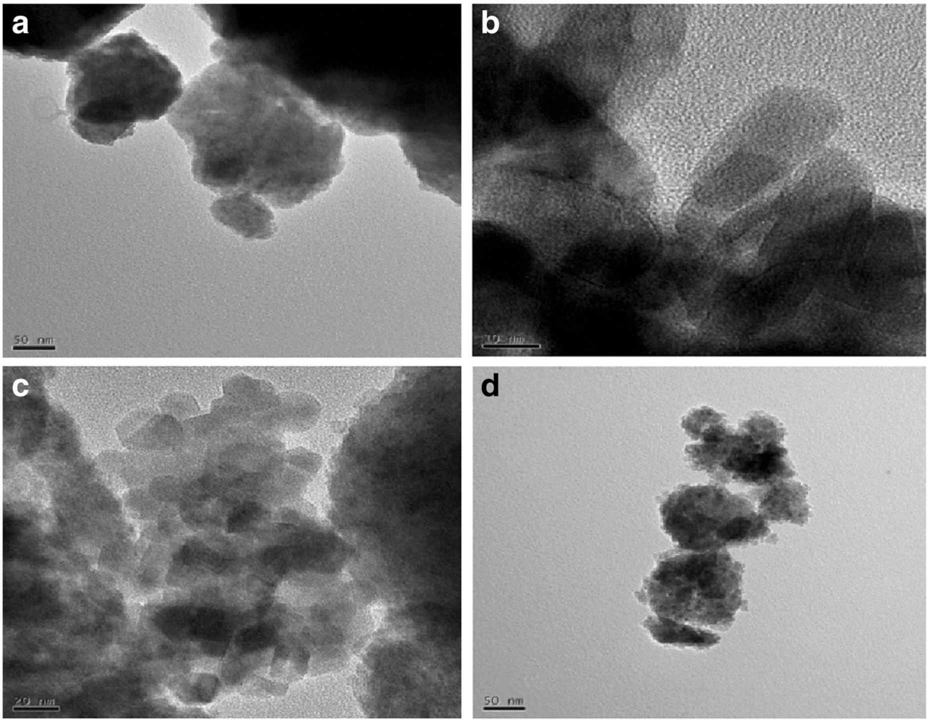

**Fig. 4** The TEM images for the four samples **a** S1, **b** S2, **c** S3, **d** S4

The average particle size determined from TEM analysis was 230 nm, which was found to be in a reasonable agreement with the figure obtained from XRD analysis.

Indeed, $^{57}$Fe Mössbauer spectrometry is highly sensitive to the superparamagnetic relaxation phenomena and consequently very powerful to study the dynamics of magnetic nanostructures, as discussed in literature [9]. The Mössbauer spectra of the four $CoFe_2O_4$ samples measured at 295 K and 78 K are shown in Fig. 5a, b respectively. All samples show two $Fe^{3+}$ well magnetically ordered sites in the crystal structure which are attributed to both tetrahedral and octahedral [10]. The spectra of the samples auto-combustion and 400 °C showed paramagnetic doublet superimposed to the two magnetic sextets with a small area ($\leq$5%), decreases to 3% at 400 °C and disappear at 600 °C and 1000 °C; indicating that the size of crystal grains grows over the superparamagnetism critical size. This critical size of superparamagnetism is about 14 nm for $CoFe_2O_4$ [11]. Table 1 shows the hyperfine interaction parameters at 295 K and 78 K (between parentheses). The isomer shift of $Fe^{3+}$ at the A-sites of $CoFe_2O_4$ increased by sintering temperature from (0.25 mm/s) for S1 to (0.29 mm/s) for S4, indicating that the electron density around $Fe^{3+}$ decreases, as a result of migration of $Co^{2+}$ ions from A-site to B-site [12, 13]. In other words, a rise of sintering temperature drives some of $Co^{2+}$ ions in A-sites to migrate to B-sites and some of $Fe^{3+}$ ions in B-sites to migrate to A-sites, leading to increase of $Fe^{3+}$ ions in A-sites. The larger hyperfine fields assigned to the B-sites is attributed to the dipolar field resulting from the deviation from cubic symmetry and also from the covalent nature of the tetrahedral bonds [14]. We expect the inter-sublattice interaction $J_{AB}$ to be stronger than the intra-sublattices $J_{AA}$ and $J_{BB}$ with $J_{AB} >> J_{BB} >> J_{AA}$ which originates from the magnetic moments of

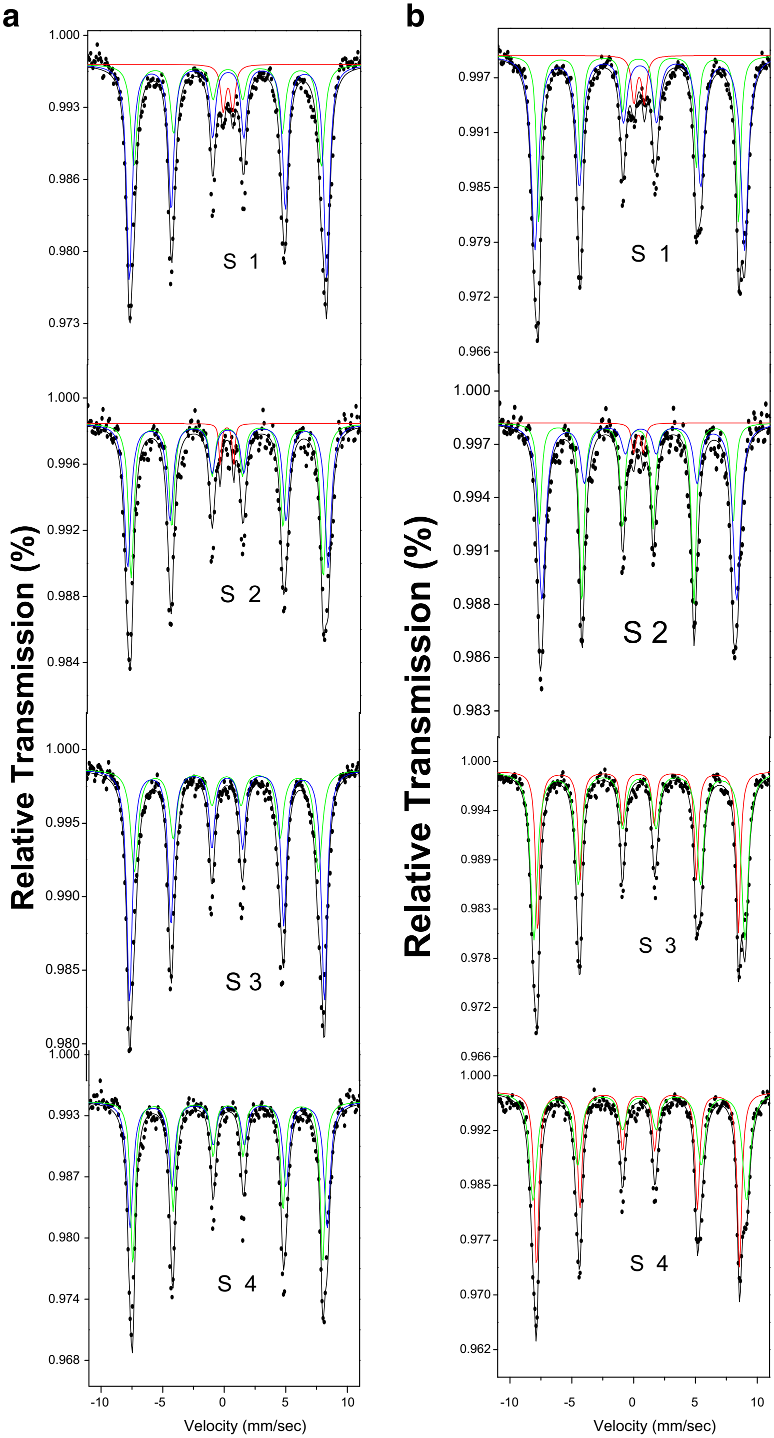

**Fig. 5** Mössbauer spectra of $CoFe_2O_4$ at **a** 295 K, **b** 78 K for the four samples

**Table 1** Mössbauer hyperfine parameters at 295 K and 78 K (between parentheses), the cation distribution and the lattice constants of $CoFe_2O_4$

| Sample | Sub-spectrum | $\delta$ (mm/s) | $\Delta E_Q{}^a$ (mm/s) | $\Gamma$ (mm/s) | $B_{hf}$ (T) | A (%) | Lattice parameter (Å) | Cation distribution (A) $[B]_2O_4$ |
|---|---|---|---|---|---|---|---|---|
| S1 | Doublet | 0.30(0.39) | 0.77(0.83) | 0.46(0.46) | –(–) | 6(5) | 8.37 | $(Co_{0.34}Fe_{0.66})$ |
| | A site | 0.25(0.34) | −0.01(0.00) | 0.42(0.42) | 46.8(50.1) | 33(32) | | $[Co_{0.66}Fe_{1.34}]_B$ |
| | B site | 0.32(0.45) | −0.01(0.00) | 0.54(0.70) | 49.3(52.6) | 61(63) | | $O_4$ |
| S2 | Doublet | 0.32(0.38) | 0.78(0.80) | 0.40(0.46) | – | 3(2) | 8.37 | $(Co_{0.26}Fe_{0.74})_A$ |
| | A site | 0.27(0.36) | −0.01(0.00) | 0.42(0.52) | 47.9(50.7) | 37(38) | | $[Co_{0.74}Fe_{1.26}]_B$ |
| | B site | 0.33(0.49) | −0.01(0.00) | 0.62(0.86) | 50.0(53.5) | 60(60) | | $O_4$ |
| S3 | A site | 0.28(0.36) | 0.00(0.00) | 0.43(0.40) | 45.9(50.3) | 45(46) | 8.37 | $(Co_{0.08}Fe_{0.92})_A$ |
| | B site | 0.34(0.46) | 0.00(0.00) | 0.72(0.60) | 48.7(52.9) | 55(54) | | $[Co_{0.92}Fe_{1.08}]_B$ |
| | | | | | | | | $O_4$ |
| S4 | A site | 0.29(0.36) | 0.0(−0.02) | 0.46(0.44) | 47.8(50.9) | 49(49) | 8.37 | $(Co_{0.02}Fe_{0.98})_A$ |
| | B site | 0.36(0.48) | 0.00(0.00) | 0.60(0.76) | 49.6(53.5) | 51(51) | | $[Co_{0.98}Fe_{1.02}]_B$ |
| | | | | | | | | $O_4$ |

The isomer shift $\delta$ (±0.02), quadrupole splitting $\Delta E_Q$ (±0.01), linewidth $\Gamma$ (±0.01), Area A (±1) are in mm/s

[a] In case of dominant magnetic interactions, $\Delta E_Q = 2\varepsilon$, where, $\varepsilon$ is a quadruple shift

the nearest neighbor cations [15]. the replacing of $Fe^{3+}$ ($5\mu_B$) with $Co^{2+}$ ($3\ \mu_B$) at the B-site causes a reduction in number of the active bonds $Fe_A$–O–$Fe_B$ which A-site $Fe^{3+}$ ions experience, and thus, the replacement within this range would not affect hyperfine magnetic field at the B-site Fe nuclei. The quadrupole splitting ($\Delta E_Q$) for both sites are nearly zero for all these spectra at 295 K and 78 K, and this is due to the increase of the surface atoms, thereby increasing in the asymmetric degree of electric distribution around $Fe^{3+}$. In case of S3, and S4 with dominant magnetic interactions, it is very important to notice that the quadrupolar shift ($2\varepsilon$) is considered instead of quadruple splitting ($\Delta E_Q$) which is characteristic of the quadrupolar electric interactions above the magnetic ordering temperature. The line width of the octahedral sites becomes broader than that of the tetrahedral sites. This broadening can be attributed to a distribution of the hyperfine fields at the A-site caused principally by a random distribution of $Fe^{3+}$ and $Co^{2+}$ ions at the B-site [16]. This becoming very clear as the sintering temperature increases; the $Fe^{3+}$ is more transfer to the tetrahedral site. The ratios of the areas under the resonance curve of the subspectra deduced from the Mössbauer measurements and the recoil free fractions of $Fe^{3+}$ at the octahedral and tetrahedral sites were used to estimate the Fe site occupancy for each site, and it is found to be 0.43, 0.59, 0.85, and 0.96 for the samples S1, S2, S3, and S4 respectively. Therefore, the calculated area ratios used to determine the cation distribution of each sample as shown in Table 1. Moreover the cation distribution shows that as the sintering temperature increases the cobalt concentration at the B-site also increases. This indicates that the synthesized sample is trying to have the inverse spinel structure at higher sintering temperatures as is the case of bulk cobalt ferrite [17].

## 4 Conclusions

Nano-crystalline cobalt ferrite has been successfully synthesized by the sol-gel auto-combustion method. XRD results confirmed the formation of cubic spinel structure in all the samples. The crystallite size of the samples increased with the higher sintering temperatures, and these samples started to crystalline after sintered it at 600 °C. The crystallite size varied from 20 to 200 nm and was in reasonable agreement with the results obtained from SEM, and TEM. The hyperfine interaction parameters obtained from the Mössbauer measurements are in a good agreement with previous published for $CoFe_2O_4$ samples. The area under resonance curve of the Mössbauer subspectra are used to derive the cation distribution of the four samples and reflected its dependence on the sintering temperature.

## References

1. Barbero, B.P., Andrade Gamboa, J., Cadús, L.E.: Synthesis and characterisation of $La_{1-x}Ca_xFeO_3$ perovskite-type oxide catalysts for total oxidation of volatile organic compounds. Appl. Catal. B **65**, 21–30 (2006)
2. Chicinas, I.: Soft magnetic nanocrystalline powders produced by mechanical alloying routes. J. Optoelectron. Adv. Mater. **8**(2), 439–448 (2006)
3. Jonker, G.H.: Analysis of the semiconducting properties of cobalt ferrite. J. Phys. Chem. Solids **9**(2), 165–175 (1959)
4. Waje, S.B., Hashim, M., Yousoff, W.D.W., Abbas, Z.: Sintering temperature dependence of room tempera-ture magnetic and dielectric properties of $Co_{0.5}Zn_{0.5}$ $Fe_2O_4$ prepared using mechanically alloyed nanoparticles. J. Magn. Magn. Mater. **322**(6), 686–691 (2010)
5. Meng, X., Li, H., Chen, J., Mein, L.: Mössbauer study of cobalt ferrite nanocrystals substituted with rare-earth $Y^{3+}$ ions. J. Magn. Magn. Mater. **321**(9), 1155–1158 (2009)
6. Sajjia, M., Oubaha, M., Hasanuzzaman, M., Olabi, A.G.: Developments of cobalt ferrite nanoparticles prepared by the sol–gel process. Ceram. Int. **40**, 1147–1154 (2014)
7. Maaz, K., Mumtaz, A., Hasanain, S.K., Ceylan, A.: J. Magn. Mater. **308**, 289–295 (2007)
8. Lu, L.T., Dung, N.T., Tung, L.D., Thanh, C.T., Quy, O.K., Chuc, N.V., Maenosonoe, S., Thanh, N.T.K.: Synthesis of magnetic cobalt ferrite nanoparticles with controlled morphology, monodispersity and composition: the influence of solvent, surfactant, reductant and synthetic conditions. Nanoscale- R. Soc. Chem. **8**, 3141–3850 (2016)
9. Greneche, J.-M.: Magnetic nanoparticles. In: Yoshida, Y., Langouche, G. (eds.) Mössbauer Spectroscopy, pp. 187–241. Springer, Berlin (2013)
10. Liu, M., Lu, M., Wang, L., Xu, S., Zhao, J., Li, H.: Mössbauer study on the magnetic properties and cationdistribution of CoFe2O4 nanoparticles synthesize by hydrothermal method. J. Mater. Sci. **51**, 5487–5492 (2016)
11. Poddar, P., Gass, J., Rebar, D.J., Srinath, S., Srikanth, H.: Magnetocaloric effect in ferrite nanoparticles. J. Magn. Magn. Mater. **307**, 227–231 (2006)
12. Iqbal, M.J., Yaqub, N., Sepiol, B., Ismail, B.: A study of the influence of crystallite size on the electrical and magnetic properties of $CuFe_2O_4$. Mater. Res. Bull. **46**, 1837–1842 (2011)
13. Singhal, S., Singh, J., Barthwal, S.K., Chandra, K.: Preparation and characterization of nanosize nickel-substituted cobalt ferrites ($Co_{1-x}Ni_xFe_2O_4$). J. Solid State Chem. **178**, 3183–3189 (2005)
14. Roumaih, Kh., Manapov, R.A., Sadykov, E.K., Pyataev, A.V.: Mössbauer studies of $Cu_{1-x}Ni_xFeMnO_4$ spinel ferrites. J. Magn. Magn. Mater. **288**, 267 (2005)
15. Subbarao, M.V., Yusuf, S.M., Kulkarni, R.G., Madhav Rao, L., Pramana, J.: Local canted spin behaviour in $Co_{1.4-x}$ $Zn_xGe_{0.4}$ $Fe_{1.2}O_4$spinels: a macroscopic, mesoscopic and microscopic study. Pramana - J. Phys. **53**, 342 (1999)
16. Fayek, M.K., Ata-Allah, S.S.: $^{57}$Fe Mössbauer and electrical studies of the (NiO)–($Cr_2O_3$) x–$(Fe_2O_3)_{2-x}$ system. Phys. Status Solidi (a) **198**, 457–464 (2003)
17. Thang, D.P., Rijnders, G., Blank, D.H.A.: Spinel cobalt ferrite by complexometric synthesis. J. Magn. Magn. Mater. **295**, 251–256 (2005)